

Non-Volatile Photochemical Gating of an Epitaxial Graphene/Polymer Heterostructure

Samuel Lara-Avila,* Kasper Moth-Poulsen, Rositza Yakimova, Thomas Bjørnholm, Vladimir Fal'ko, Alexander Tzalenchuk, and Sergey Kubatkin

Graphene, a single layer of carbon atoms, is steadily making inroads into the applications that presently rely on semiconductor heterostructures.^[1] Recent advances include high frequency analogue transistors and a quantum Hall resistance standard based on wafer scale epitaxial graphene on silicon carbide (SiC).^[2–4] Interaction with the SiC substrate causes strong and often non-uniform electron doping of graphene, imposing constraints on device engineering. Further progress depends on the ability to control the electrical parameters of the material, such as the charge density or its resistance, in a non-volatile way.

Analogous to semiconductor non-volatile memory devices,^[5,6] we demonstrate non-invasive carrier density control in a special graphene–polymer heterostructure exposed to UV light. In this way, we have achieved up to 50 times compensation of the substrate-induced electron density, with the carrier mobility rising above $16\,000\text{ cm}^2\text{ V}^{-1}\text{ s}^{-1}$ at 4.2 K. This corresponds to about an order of magnitude increase in the device resistance in the irradiated state. The electronic properties of the exposed SiC/graphene/polymer heterostructures remained stable over many days at room temperature, but heating the polymers to above the glass transition reversed the effect of light. Unexposed, the same double layer of polymers works well as a cap layer,

improving the temporal stability and uniformity of doping levels of the sample.

Additionally, we identify the growth conditions that reliably produce monolayer graphene with a carrier density below the critical value, $n_c \approx 10^{13}\text{ cm}^{-2}$,^[7] enabling electrostatic control of the charge carrier density.

Methods for precise control of the carrier density in electronic materials are the cornerstone of modern semiconductor technology. Chemical methods ranging from direct doping to modulation doping have been substantially refined for semiconductors over the last half-century; once doped, the carrier density in a semiconductor can be further tuned by applying an electric field produced by a charged gate, as in field-effect transistors.

Carrier control by field effect is non-invasive, since it does not introduce additional scattering by charged impurities, but it requires an external voltage source permanently connected to the gate. An alternative approach for carrier control comes from semiconductor programmable non-volatile memory devices, in which the carrier density of materials can be changed, frozen, and then erased. These devices are essentially transistors with one extra floating, isolated gate placed between the control gate and the semiconductor channel. Charge can be transferred to the floating gate by an electric pulse on the control gate and stored there almost infinitely (write operation), until intentionally leaked through the dielectric, e.g., activated by UV light (erase operation). In other implementations of the non-volatile memory devices UV light is used for writing, in which case thermal activation can be used for erasing.^[5,6]

Carrier density control in graphene, a zero-bandgap semiconductor, has been demonstrated successfully by direct chemical doping and also by an electric field. However, any direct contact to the graphene monolayer with either intentionally or unintentionally introduced chemical dopants (such as adsorbates or interface defects) or inorganic gate insulators increases scattering and thus reduces the mobility of the charge carriers in the material. Therefore, methods of non-invasive, non-volatile, and reversible charge carrier control would be particularly important for device engineering based on large-scale epitaxial graphene, which is often heavily and unpredictably electron-doped through interaction with the substrate.^[1]

In order to circumvent this problem we engineered a graphene-polymer heterostructure (**Figure 1a**) by coating the graphene with poly(methylmethacrylate-*co*-methacrylate acid), henceforth PMMA/MMA (**Figure 1b**), followed by poly(methyl styrene-*co*-chloromethyl acrylate), hereafter ZEP520A (**Figure 1c**). The ZEP520A layer, chosen for its ability to provide potent acceptors under deep UV light, acts as a floating gate, while the

S. Lara-Avila, Prof. S. Kubatkin
Department of Microtechnology and Nanoscience
Chalmers University of Technology
Göteborg, S-41296, Sweden
E-mail: samuel.lara@chalmers.se

Dr. K. Moth-Poulsen
College of Chemistry
University of California, Berkeley
Berkeley, CA 94720, USA

Prof. R. Yakimova
Department of Physics
Chemistry and Biology (IFM)
Linköping University
Linköping, S-581 83, Sweden

Prof. T. Bjørnholm
Nano-Science Center and Department of Chemistry
University of Copenhagen
Copenhagen, DK-2100 ø, Denmark

Prof. V. Fal'ko
Physics Department
Lancaster University
Lancaster, LA1 4YB, UK

Prof. A. Tzalenchuk
National Physical Laboratory
Teddington, TW11 0LW, UK

DOI: 10.1002/adma.201003993

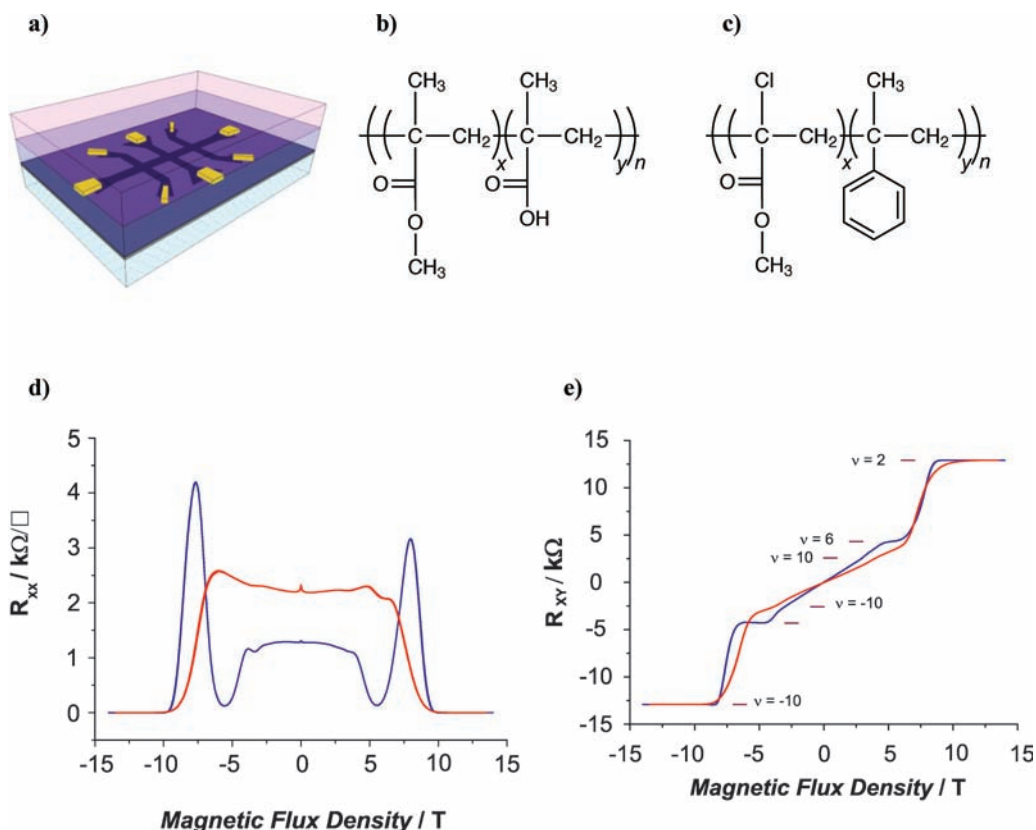


Figure 1. a) Layout of the SiC/graphene/polymer heterostructure (dark blue layer = PMMA/MMA; violet layer = ZEP520A). b) Chemical structure of the spacer layer, poly(methylmethacrylate-co-methacrylate acid). c) Chemical structure of the top, active layer, poly(methyl styrene-co-chloromethyl acrylate), ZEP520A. Magnetotransport measurements showed that a mere encapsulation of graphene ($160 \times 35 \mu\text{m}$ Hall bar) enhanced its temporal stability and transport characteristics, as manifested through the d) longitudinal and d) Hall resistances; red lines correspond to the unprotected sample, blue lines to the same sample covered by the double layer of polymers. Quantum Hall plateaus are marked in (e).

use of a PMMA-based copolymer as a spacer layer is justified by its ability to preserve the electrical properties of graphene,^[8] such as the carrier mobility, well-known to deteriorate in contact with inorganic dielectrics.^[9]

The experiments indicate that electron acceptors are present in small numbers in the pristine polymers and even a mere encapsulation of the sample (spin-coating graphene with PMMA/MMA+ZEP520A) resulted in a reduced electron density (10–40%), significantly improved electron mobility (50%), higher charge density uniformity, and better temporal stability.

The effect of encapsulation was studied through low-temperature ($T = 4.2$ K) magnetotransport measurements on the graphene sample thoroughly investigated in its pristine form in Ref. [3]. The longitudinal sheet resistance (R_{xx}) and transversal resistance (R_{xy}) are presented in Figure 1d,e, respectively, before (blue) and after (red) encapsulation; from these measurements it was found that upon encapsulation the carrier density, calculated as $n = B/(eR_{xy})$, with the electron charge $e = 1.60 \times 10^{-19}$ C, at a magnetic flux density $B = 1$ T, dropped from $1.1 \times 10^{12} \text{ cm}^{-2}$ to $n = 7.8 \times 10^{11} \text{ cm}^{-2}$, and this was accompanied by an increment in the carrier mobility from $2640 \text{ cm}^2 \text{ V}^{-1} \text{ s}^{-1}$ to $6340 \text{ cm}^2 \text{ V}^{-1} \text{ s}^{-1}$.

Figure 1d,e show that despite displaying quantum Hall effect, the pristine sample exhibited spatial inhomogeneities of the charge density manifested as a parabolic background

in R_{xx} near zero magnetic field and smeared Shubnikov-de Haas (SdH) oscillations and quantum Hall plateaus. The encapsulated sample, on the other hand, displayed a flat background in R_{xx} near zero field, enhanced SdH oscillations, and sharper quantum Hall plateaus at filling factors $\nu = 2, 6$, and 10 , revealing the true monolayer nature of the sample.^[10] The electronic properties of the encapsulated sample persisted after prolonged exposure to the environment over a year time period during which the sample was subjected to more than ten thermal cycles between 300 mK and room temperature. Along this time only a slow, but steady reduction in the electron density was observed, presumably due to a small number of uncontrolled acceptors appearing in the ZEP520A layer.

A single PMMA/MMA layer did not give any such improvement, in line with previous observations for exfoliated graphene, where it was found that rendering the substrate hydrophobic with subsequent encapsulation using a polymer protects exfoliated graphene from water adsorption and leads to only minor deterioration of charge mobility.^[8,11] Altogether, these findings show that encapsulation resulted in a significantly more uniform distribution of charge density in the sample, lower carrier concentration, and enhanced mobility.

Not surprisingly, the relatively low density in the as-produced graphene samples could be further reduced, at least 4 times, using a metallic gate in a control experiment where the

ZEP520A layer was replaced by a metallic gate deposited on the PMMA/MMA layer. The carrier density was determined from measurements of the Hall resistance R_{xy} (Figure 2a) at the magnetic flux density $B = 0.5$ T and plotted in Figure 2b,c (black squares). In this case the charge transfer to the gate, $n_g = CV_g/e$, where V_g is the gate voltage and C is the gate capacitance to graphene per unit area determined by the geometry and the properties of the gate dielectric. The maximum n_g was limited by the breakdown of the dielectric near $V_g = -60$ V.

After verifying that PMMA/MMA works well as a spacer layer and that the carrier concentration in the graphene samples could be efficiently modulated by an electrostatic field, the graphene/PMMA/MMA/ZEP520A heterostructure was exposed to deep UV light to demonstrate photochemical gating of graphene, which is conceptually different from the direct chemical doping, where the dopants are sitting directly on top of graphene.^[8,12,13] In a sample with the initial carrier

density $n \approx 10^{12}$ cm⁻², subsequent exposures to UV at a 248 nm wavelength up to the dose of 330 mJ cm⁻² decreased the low-temperature electron density by 50 times down to 2×10^{10} cm⁻² (Figure 2b,c, blue circles), lowering the onset field of the $\nu = 2$ quantized resistance plateau to magnetic flux densities below 1 T (Figure 2d). Exposure resulted in a fivefold increment in carrier mobility up to 16 000 cm² V⁻¹ s⁻¹ (Figure 2c, blue circles) and tenfold increment in the resistance of graphene. The irradiated devices remained latched in their high-resistance state over many days. The on/off ratio of 10 for the resistance of the photochemically gated devices is similar to the best large-area single-layer graphene transistors demonstrated to-date.^[14] Very significantly, annealing the samples at 170 °C, just above the glass transition temperature of the polymers, reversed the effects of light and returned the graphene charge carrier density to its value prior to UV exposure. A subsequent UV exposure with a dose of 30 mJ cm⁻² again decreased the density

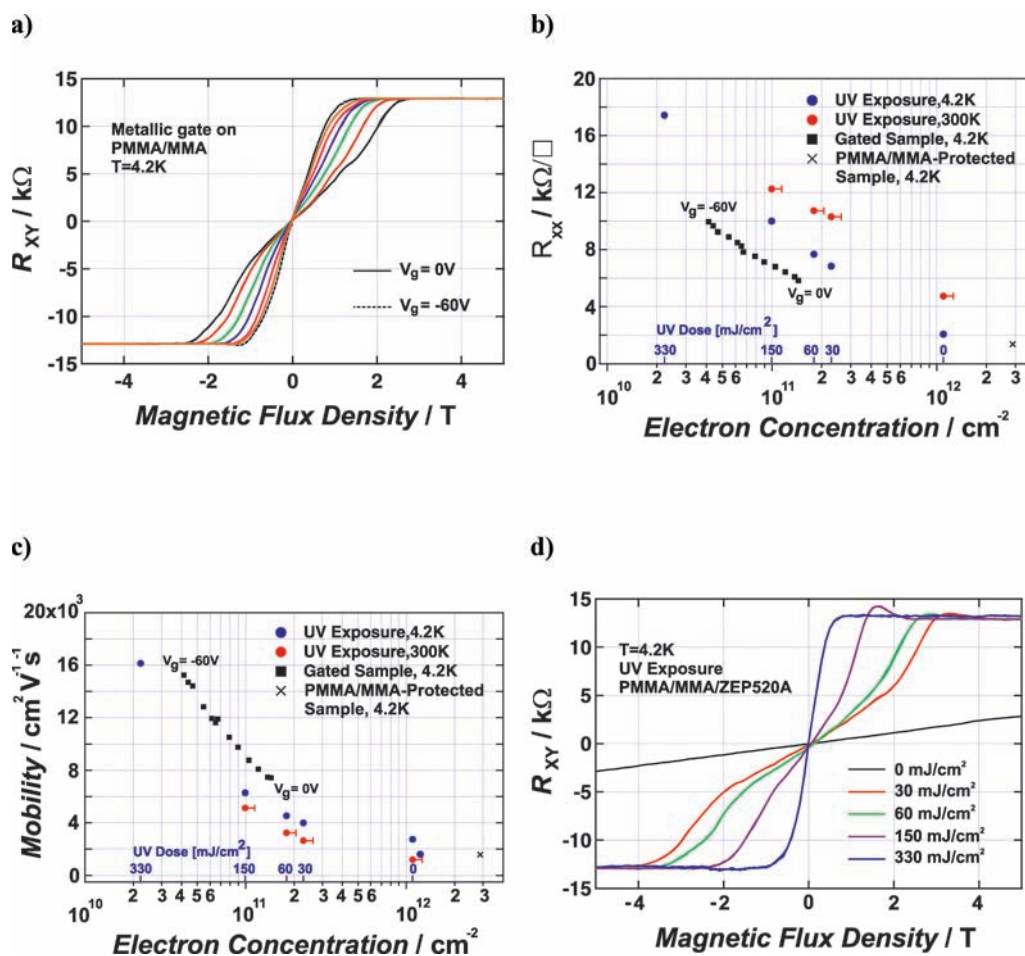


Figure 2. a) Hall resistance measurements demonstrating the electrostatic control of carrier concentration for different gate voltages ($V_g = 0$ to $V_g = -60$ V in steps of -10 V) in the electrically gated device. As the carrier density in graphene is decreased, the onset of the $\nu = 2$ quantum Hall plateau is pushed down in magnetic flux density (b). c) Direct comparison of the electrostatic and photochemical gating effect on the resistivity and the carriers mobility; the electron concentration has been obtained from the measured Hall resistance as $n = B/(eR_{xy})$ at $B = 0.5$ T. Note that for each UV dose the carrier density measured at room temperature was consistently higher than that at 4.2 K by 10–15%. The error bars on the room temperature data points reflect this discrepancy, which may be caused by thermal excitations. d) Hall resistance measurements for different UV exposure doses in the photochemically gated device, demonstrating a steady decrease of the carrier density, lowering the onset field of the $\nu = 2$ quantized resistance plateau to magnetic flux densities below 1 T.

8 times, confirming at least partial reversibility of the UV doping procedure. The behavior at room temperature was the same as the one observed at low temperatures (Figure 2c, red circles); similar characteristics were observed in all studied samples. A possible way to further improve the reversibility of the photochemical gating could be by carefully designing the polymers to be used in the graphene/polymer heterostructure.

The light-induced effects can be understood by considering the photochemistry of the polymers in this heterostructure. It is known that both PMMA/MMA and ZEP520A polymers undergo a photoinduced scission-type reaction when exposed to an electron beam or UV light.^[15,16] The mechanism (Figure 3a) for the ZEP520A polymer predominantly proceeds via an initial homolytic bond cleavage of the C–Cl bond into a neutral Cl radical and a neutral carbon radical.^[17] The result is the formation of a photoinduced abundance of Cl radicals that are potent electron acceptors. Since PMMA/MMA does not possess any Cl, this mechanism cannot take place, as verified in a control experiment, where the graphene sample protected with only 330 nm of PMMA/MMA and no ZEP520A was exposed to UV light with a dose of 30 mJ cm⁻². The outcome was a mere 3 times increase in the electron density, confirming that ZEP520A is the layer responsible for providing electron acceptors and suggesting that a small number of levels produced by the UV exposure in PMMA/MMA work effectively as electron donors. We emphasize that the above description, summarized in Figure 3b, represents a likely scenario describing the initial step of a process that explains the experimental observation.

In the process of photochemical gating the amount of charge transfer, n_g is controlled by two parameters: n_a , the number of available acceptors in ZEP520A and A_g , the difference in the work functions between the graphene layer and the electrons in the acceptor layer (ZEP520A). During the light-induced charge transfer in the heterostructure, A_g is reduced by the electric field potential building up across the spacer layer, limiting in this way the number of filled acceptors. This qualitative description of the charge transfer process in the heterostructure

is supported by a more rigorous analysis in Ref. [7] (see also the Supporting Information). Experimentally, the amount of charge transfer from graphene to the ZEP520A layer, n_g , follows the relation $n_g = \min\{n_a, CA_g/e^2\}$. In the limit when acceptors were abundant, a thinner PMMA/MMA spacer (down to 50 nm) led to a proportionally stronger effect of illumination (by increasing C), though for even thinner PMMA/MMA layers or with ZEP520A deposited straight on graphene we observed a reduction in mobility, emphasizing the role of the PMMA/MMA spacer in separating the mobile electrons in graphene from the charged scatterers in ZEP520A. In the opposite limit corresponding to a large CA_g/e^2 , a thicker active ZEP520A layer led to a larger achievable shift in n_g by increasing the number of available acceptors, indicating that the bulk of the ZEP520A layer is responsible for the photochemical gating and it is not caused by the interface between the polymers.

The possibility to control the carrier density by either electrostatic field or photochemical gating in these samples stems from the low initial carrier concentration in the as-produced graphene. According to the analysis of the charge transfer between the graphene and the donors in SiC,^[7] there is an upper limit on the gate controllable charge carrier concentration $n_* \approx 1 \times 10^{13}$ cm⁻². Graphene, which has a higher carrier density, has a Fermi level pinned by impurities, making the carrier density control in epitaxial graphene inefficient. The graphene samples studied in our experiments have been grown on the Si-terminated face of a semi-insulating 4H–SiC(0001) substrate (Cree Inc.) at 2000 °C and 1 atm Ar gas pressure, which resulted in monolayers of graphene that were atomically uniform over more than 50 μm², as shown by low-energy electron microscopy. These conditions reliably produced a carrier density of $n \approx 10^{12}$ cm⁻², which is much lower than n_* . We speculate that high-temperature annealing of SiC compensates the surface donor states, possibly through surface segregation of impurities (e.g., B or N) abundant in bulk SiC crystals, or merely reduction of the number of surface defects.

In summary, we have demonstrated a novel heterostructure based on epitaxial graphene grown on silicon carbide combined with two polymers: a neutral spacer and a photoactive layer that provides potent electron acceptors under UV light exposure. This method enables control of the electrical parameters of graphene in a non-invasive, non-volatile, and reversible way.

The newly developed photochemical gating has already helped us to improve the robustness (large range of quantizing magnetic field, substantially higher operation temperature and significantly enhanced signal-to-noise ratio due to significantly increased breakdown current) of a graphene resistance standard to such a level that it starts to compete favorably with mature semiconductor heterostructure standards.^[3,18] SiC/graphene/polymer heterostructures could open an attractive application of graphene as a true “monolithic” electronic material suitable for making integrated solid-state circuits, by selectively exposing to UV those areas of the heterostructure where the carrier

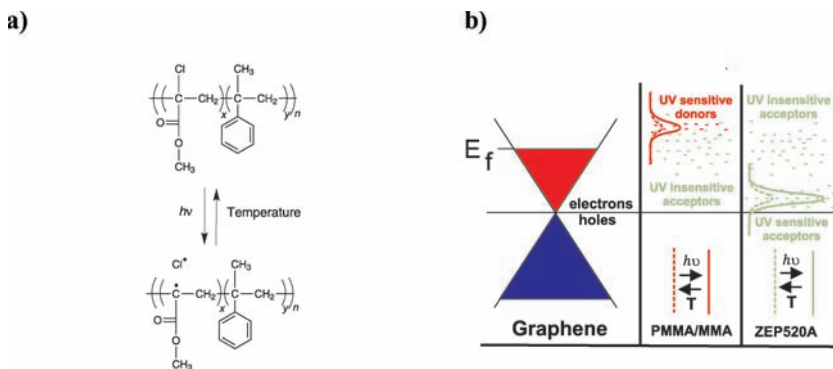


Figure 3. a) Photoinduced scission-type mechanism for ZEP520A exposed to UV light; homolytic bond cleavage of the C–Cl bond due to UV exposure results in photoinduced abundance of Cl radicals, which are potent electron acceptors. b) Schematic band diagram of the SiC/graphene/polymer heterostructure, where the polymer is a bilayer of PMMA/MMA+ZEP520A. Donors (red dashes) and acceptors (green dashes) are already present in the pristine polymers. Exposure to UV increases the concentration of donors in PMMA/MMA to some extent and acceptors in ZEP520A to a greater amount (solid lines). Heating the heterostructure to temperatures above the glass transition of the polymers partially restores the original donor concentration in PMMA/MMA and acceptors in ZEP520A (dashed lines).

density has to be modulated. In the heterostructures presented in this report, the observed variation in resistance was tenfold upon 50 times variation of the carrier density by photochemical gating, and the on/off ratio of the SiC/graphene/polymer device could be further improved by using bilayer graphene (BLG), which has a great advantage determined by its peculiar spectrum: a transverse electric field opens an interlayer asymmetry gap for electrons in BLG.^[19–22] For structures with initial density $n \approx 10^{12} \text{ cm}^{-2}$, such a gap in a device driven to the neutrality point by photochemical gating can be estimated as $\Delta \approx 10 \text{ meV}$,^[23] sufficiently high to modulate the room-temperature conductivity.^[24] We also foresee applications as sensors, where the polymer in the heterostructure can be sensitized to respond not only to light but to a specific stimulus, which leads to a change in the conductance of the underlying graphene. To this end, the reported results should be regarded as an exploratory demonstration of a technological opportunity; more generally, the work connects the young and rapidly developing field of graphene electronics and the mature field of organic electronics.

Experimental Section

Hall Bar Fabrication: Hall bar devices of different sizes, from $160 \mu\text{m} \times 35 \mu\text{m}$ to $11.6 \mu\text{m} \times 2 \mu\text{m}$, were produced on several wafers using standard electron beam lithography and oxygen plasma etching. Atomic force microscopy (AFM) images reveal that the graphene layer in all devices crossed the substrate steps. Contacts to graphene were produced by straightforward deposition of 3 nm Ti and 100 nm Au through a lithographically defined mask followed by lift-off.

Encapsulation and UV Exposure: All samples were thoroughly cleaned in acetone and isopropyl alcohol prior to encapsulation. The polymer used for the spacer layer was the positive electronbeam resist poly(methylmethacrylate-co-methacrylate acid), commercially known as PMMA/MMA (MMA (8.5) MAA) (Microchem Corp.). Our normal spin-coating procedure produced a 330-nm-thick layer. The polymer was baked at 170 °C for 5 min. The polymer used for the top, active layer was 300-nm-thick poly(methyl styrene-co-chloromethyl acrylate), traded as ZEP520 (Nippon Zeon Co., Ltd); it was also baked at 170 °C for 5 min. Any further baking resulted in slight increase in electron density by $\approx 1 \times 10^{11} \text{ cm}^{-2}$. The exposure to UV was carried out in a mask aligner equipped with a 248-nm mercury lamp with a power density of 1.5 mW cm^{-2} . Each exposure was followed by magnetoresistance measurements at $T = 4.2 \text{ K}$ and fields up to 5 T.

Supporting Information

Supporting Information is available from the Wiley Online Library or from the author.

Acknowledgements

This work was supported by the NPL Strategic Research Programme, Swedish Research Council and Foundation for Strategic Research,

EU FP7 STREPs “Concept Graphene” and SINGLE, EPSRC grant EP/G041954, and the Science & Innovation Award EP/G014787. K.M.-P. acknowledges the Danish Research Councils for funding via the grant 2009 09 – 066585/FNU. The authors would like to thank F. Lombardi, A. Danilov, J. T. Janssen, and T. Claeson for illuminating discussions; A. Kalabukhov for help with experiments; and T. Nannestad and H. Weihe for EPR spectroscopy.

Received: October 28, 2010

Published online: January 7, 2011

- [1] A. K. Geim, *Science* **2009**, *324*, 1530.
- [2] Y. M. Lin, K. A. Jenkins, A. Valdes-Garcia, J. P. Small, D. B. Farmer, P. Avouris, *Nano Lett.* **2009**, *9*, 422.
- [3] A. Tzalenchuk, S. Lara-Avila, A. Kalabukhov, S. Paolillo, M. Syvajarvi, R. Yakimova, O. Kazakova, T. J. B. M. Janssen, V. Fal'ko, S. Kubatkin, *Nat. Nanotechnol.* **2010**, *5*, 186.
- [4] P. N. First, W. A. de Heer, T. Seyller, C. Berger, J. A. Stroscio, J. S. Moon, *MRS Bull.* **2010**, *35*, 296.
- [5] L. A. Glasser, in *Chapel Hill Conference on VLSI*, (Ed: H. Fuchs), Computer Science Press, Chapel Hill, NC, USA **1985**, 61.
- [6] D. A. Kerns, J. Tanner, M. Sivillotti, J. Luo, in *Proceedings of the 1991 University of California/Santa Cruz Conference on Advanced Research in VLSI*, (Ed: C. H. Séquin), MIT Press, Cambridge, MA, USA **1991**, 245.
- [7] S. Kopylov, A. Tzalenchuk, S. Kubatkin, V. I. Fal'ko, *Appl. Phys. Lett.* **2010**, *97*, 112109.
- [8] T. Lohmann, K. von Klitzing, J. H. Smet, *Nano Lett.* **2009**, *9*, 1973.
- [9] D. B. Farmer, H. Y. Chiu, Y. M. Lin, K. A. Jenkins, F. N. Xia, P. Avouris, *Nano Lett.* **2009**, *9*, 4474.
- [10] A. H. Castro Neto, F. Guinea, N. M. R. Peres, K. S. Novoselov, A. K. Geim, *Rev. Mod. Phys.* **2009**, *81*, 109.
- [11] M. Lafkioti, B. Krauss, T. Lohmann, U. Zschieschang, H. Klauk, K. von Klitzing, J. H. Smet, *Nano Lett.* **2010**, *10*, 1149.
- [12] J. Jobst, D. Waldmann, F. Speck, R. Hirner, D. K. Maude, T. Seyller, H. B. Weber, *Phys. Rev. B* **2010**, *81*, 195434.
- [13] K. Brenner, R. Murali, *Appl. Phys. Lett.* **2010**, *96*, 063104.
- [14] F. Schwierz, *Nat. Nanotechnol.* **2010**, *5*, 487.
- [15] T. Nishida, M. Notomi, R. Iga, T. Tamamura, *Jpn. J. Appl. Phys.* **1992**, *31*, 4508.
- [16] K. K. Okudaira, E. Morikawa, S. Hasegawa, P. T. Sprunger, V. Saile, K. Seki, Y. Harada, N. Ueno, *J. Electron Spectrosc. Relat. Phenom.* **1998**, *88*, 913.
- [17] H. Ikeura-Sekiguchi, T. Sekiguchi, M. Koike, *J. Electron Spectrosc. Relat. Phenom.* **2005**, *144*, 453.
- [18] T. J. B. M. Janssen, A. Tzalenchuk, R. Yakimova, S. Kubatkin, S. Lara-Avila, S. Kopylov, V. Fal'ko, arXiv:1009.3450v2 **2010**.
- [19] E. McCann, V. I. Fal'ko, *Phys. Rev. Lett.* **2006**, *96*, 086805.
- [20] T. Ohta, A. Bostwick, T. Seyller, K. Horn, E. Rotenberg, *Science* **2006**, *313*, 951.
- [21] J. B. Oostinga, H. B. Heersche, X. L. Liu, A. F. Morpurgo, L. M. K. Vandersypen, *Nat. Mater.* **2008**, *7*, 151.
- [22] Y. B. Zhang, T. T. Tang, C. Girit, Z. Hao, M. C. Martin, A. Zettl, M. F. Crommie, Y. R. Shen, F. Wang, *Nature* **2009**, *459*, 820.
- [23] E. McCann, *Phys. Rev. B* **2006**, *74*, 161403.
- [24] B. N. Szafrank, D. Schall, M. Otto, D. Neumaier, H. Kurz, *Appl. Phys. Lett.* **2010**, *96*, 112103.